Article

Chinese Science Bulletin

Geology

March 2012 Vol.57 No.9: 1024–1035
doi: 10.1007/s11434-011-4968-z

Indosinian isotope ages of plutons and deposits in southwestern Miaoershan-Yuechengling, northeastern Guangxi and implications on Indosinian mineralization in South China

WU Jing[1], LIANG HuaYing[1*], HUANG WenTing[1,5], WANG ChunLong[1,5], SUN WeiDong[1], SUN YaLi[2], LI Jing[1,3], MO JiHai[4] & WANG XiuZhang[1]

[1] *CAS Key Laboratory of Mineralogy and Metallogeny, Guangzhou Institute of Geochemistry, Chinese Academy of Sciences, Guangzhou 510640, China;*
[2] *State Key Laboratory of Isotope Geochemistry, Guangzhou Institute of Geochemistry, Chinese Academy of Sciences, Guangzhou 510640, China;*
[3] *Zijin Mining Group Company Limited, Xiamen 364200, China;*
[4] *Guangdong Nuclear Industry Bureau, Guangzhou 510800, China;*
[5] *Graduate University of Chinese Academy of Sciences, Beijing 100049, China*

Received October 9, 2011; accepted December 28, 2011; published online January 31, 2012

The Miaoershan-Yuechengling complex pluton is the largest granitoid complex in the western Nanling metallogenic belt with a surface exposure of >3000 km^2. The complex pluton is composed of an early stage granitoid batholith and late stage small intrusions. The early stage batholith contains mainly medium-grained porphyritic mica granite and porphyritic monzonite granite, whereas the late stage intrusions are composed of muscovite granite porphyry and muscovite monzonitic granite. There are many W-Sn-Mo-Pb-Zn-Cu ores in the contact zone between the batholith and strata, forming an ore-rich belt around the batholith. Based on zircon LA-ICP-MS U-Pb ages, the southwestern part of the early stage batholith formed at 228.7 ± 4.1 Ma (MSWD = 2.49), with slightly earlier magmatic activity at 243.0 ± 5.8 Ma (MSWD = 2.62). The Yuntoujie muscovite granite was associated with W-Mo mineralization and has a zircon LA-ICP-MS U-Pb age of 216.8 ± 4.9 Ma (MSWD = 1.44). The Re-Os isochron age of molybdenite from the Yuntoujie W-Mo ore was 216.8 ± 7.5 Ma (MSWD = 11.3). Our new isotope data suggest that the late stage intrusive stocks from the southwestern Miaoershan-Yuechengling batholith were closely associated with W-Mo mineralization from the Indosinian period. These new results together with previous isotope data, suggest that South China underwent not only the well-known Yanshanian mineralization event, but also a widespread Indosinian metallogenic event during the Mesozoic period. Therefore, South China has a greater potential for Indosinian mineralization than previously thought such that more attention should be given to the Indosinian ore prospecting in South China.

Nanling metallogenic belt, ore genesis, isotope age, W-Mo deposit, Indosinian

Citation: Wu J, Liang H Y, Huang W T, et al. Indosinian isotope ages of plutons and deposits in southwestern Miaoershan-Yuechengling, northeastern Guangxi and implications on Indosinian mineralization in South China. Chin Sci Bull, 2012, 57: 1024–1035, doi: 10.1007/s11434-011-4968-z

The Nanling metallogenic ore belt is well known for its W-Sn-Be-Nb-Ta-REE mineralization and has attracted much attention from geoscientists worldwide. A large amount of the work from South China has examined the temporal and spatial distributions of the granitoids and their associated mineralizations [1–26]. Most of that work focuses on the granitoids and related deposits in the middle and the eastern parts of the Nanling ore belt, whereas there is less research from the western part of Nanling ore belt. South China underwent both Indosinian and Yanshanian structural-magmatic events with more focus on the Yanshanian stage mineralization. The Miaoershan-Yuechengling complex pluton is the largest granitoid pluton outcrop in the western Nanling metallogenic belt. Many W-Sn (Mo) and Pb-Zn-Cu deposits

*Corresponding author (email: lianghy@gig.ac.cn)

occurred in the contact zone between the complex pluton and the adjacent strata, forming an ore rich belt around the complex pluton. However, little work has been done on the complex pluton and its adjacent deposits. For example, the ages of the complex pluton are not well constrained. Most researchers proposed that it was formed during the Galedonian period [10] whereas others argue it was emplaced during the Indosinian or Yanshanian periods [27,28]. The ages of these deposits from around the contact zone between the complex pluton and adjacent strata have not yet been reported. Precise dating of the complex pluton and adjacent deposits is very important for understanding the relationship between the evolution of the melts and the formation of the deposits and also for examining the formation processes of the whole Nanling ore belt. This study presents a new zircon laser ablation plasma mass spectrometry (LA-ICP-MS) U-Pb ages and molybdenite Re-Os ages of the batholith and adjacent W-Mo deposit, respectively. We also discuss the Indosinian mineralization associated with granite from South China.

1 Geological setting

The Miaoershan-Yuechengling complex pluton has a surface area of more than 3000 km^2 and is the largest scale granitoid pluton in the western Nanling metallogenic belt. The granitoid pluton is characterized by an elliptical shape on the surface and is located in the axial plane of an anticline. The long axis of the pluton is concordant with the trend of the anticline in the region (Figure 1). The Miaoershan-Yuechengling complex pluton comprises of multiphase intrusions dominated by an early stage batholith and late stage intrusions. Late stage intrusions occurred mainly as smaller intrusions, dikes, or stocks, which are located mainly in the batholith and its adjacent contact zone. Many deposits of W-Sn-Mo-Pb-Zn-Cu have been found surrounding the contact zone between the complex pluton and strata, forming an ore rich belt around the complex pluton (Figure 1).

The study area is located at the southwestern part of the complex pluton (Figure 1). Early stage batholith samples were collected at the gate of an underground derivation

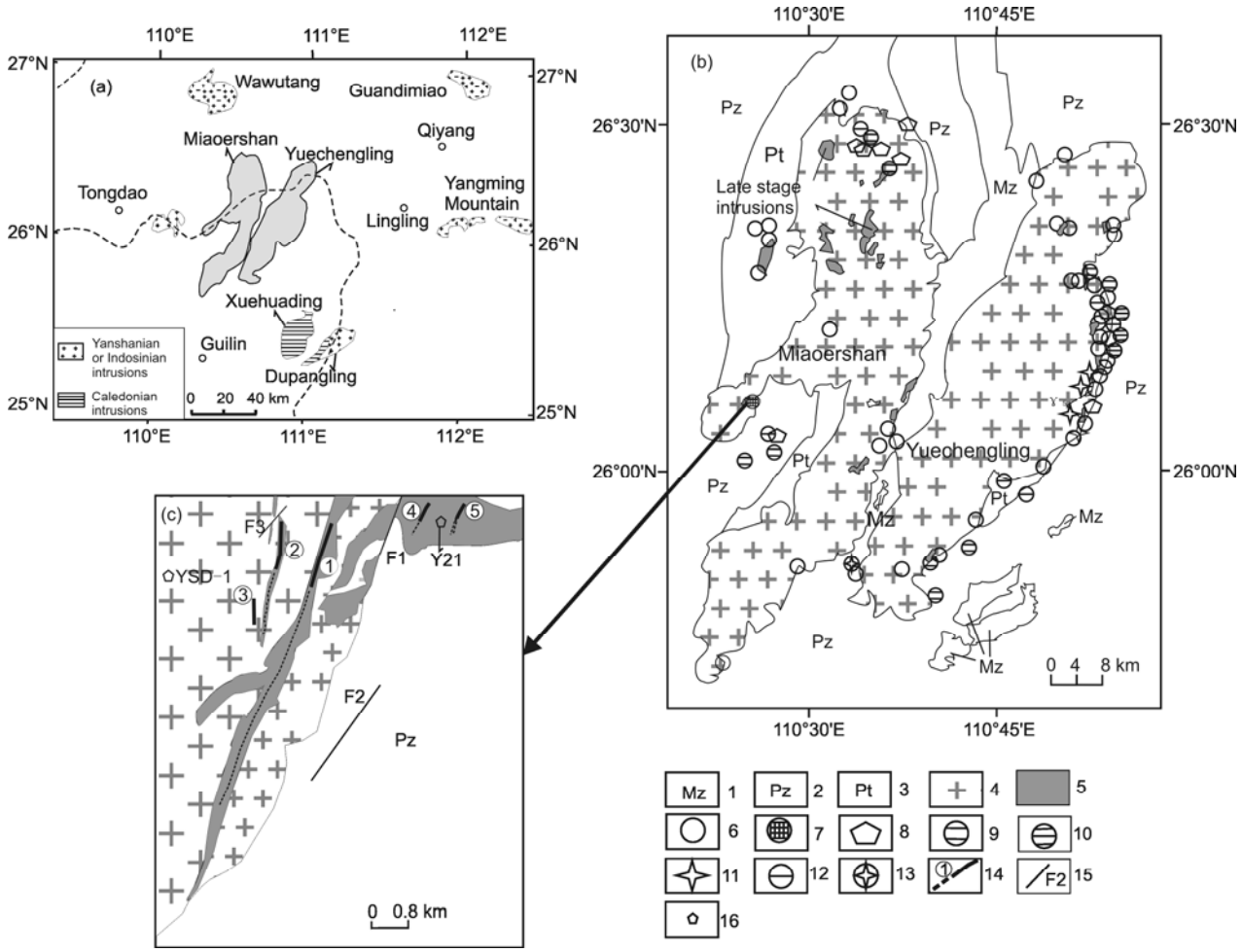

Figure 1 Simplified geological map showing the location of the Miaoershan-Yuechenling complex plution (a), geology (b) and Yuntoujie W-Mo deposit (c). 1, Mesozoic strata; 2, Paleozoic strata; 3, Proterozoic strata; 4, early stage batholiths; 5, late stage intrusion; 6, W deposit (occurrence); 7, W-Mo deposit (occurrence); 8, Cu deposit (occurrence); 9, Pb-Zn deposit (occurrence); 10, poly-metal deposit (occurrence); 11, Sn deposit (occurrence); 12, Pb deposit (occurrence); 13, W-Sn deposit (occurrence); 14, number of the constrained or suggested ore bodies; 15, fault; 16, sample locality.

tunnel located at 26°04′11.5″N, 110°24′20.2″E in the southwestern rim of the Miaoershan-Yuechenling complex pluton. Based on observations within the 2 km long derivation tunnel and along the 2 km long surface profile, the early stage batholith is composed mainly of middle-grained porphyritic biotite granite and some middle-grained porphyritic biotite monzonite granite. The early stage batholith displays massive structure and a porphyritic texture. The phenocrysts have grain sizes of >2 mm and matrices with grain sizes <2 mm are similar in mineralogy. For example, plagioclase = 22%–27%, K-feldspar = 32%–34%, quartz = 33%–39%, biotite = 8%–11% with accessory minerals such as zircon, apatite and monazite.

Late stage samples were collected from the Yuntoujie late stage (26°03′48″N, 110°23′01″E). This consisted of an ore bearing intrusion that occurred in the southwestern part of the Miaoershan-Yuechenling complex batholith. The Yuntoujie late stage W-Mo ore bearing intrusion occurred in the early stage batholith and the contact zone between the batholith and strata. A chilled contact was observed between the early stage batholith and the late stage intrusion (Figure 2), suggesting that late stage magma was emplaced after the crystallization and cooling of the early stage batholith. The late stage intrusion is composed mainly of fine-grained muscovite monzonite granite porphyry, fine-grained tourmaline muscovite granite porphyry, and medium-grained muscovite granite. The late stage intrusion is a white color, massive structure, porphyritic and of granular texture. The porphyritic granite has muscovite, plagioclase and quartz phenocrysts with grain sizes of >2.5 mm set in a medium-grained phanerocrystalline matrix of similar mineralogy. The late stage muscovite granite is composed of perthite (19%–27%), plagioclase (19%–27%), quartz (32%–50%), muscovite (4%–8%) with minor biotite, and accessory minerals such as zircon.

The Yuntoujie W-Mo ore is a middle size deposit, with an estimated W metal reserve of approximately 10000 t. The Yuntoujie W-Mo deposit has vein and veinlet mineralization that occurs in the late stage granite. Five ore bodies have been found in the Yuntoujie ore field [29]. These ore-bodies were 200 to 1000 m in length, with widths varying from 20 to 30 cm [29]. The Yuntoujie W-Mo deposit is characterized by zoning of mineralization, with wolframite, scheelite, and molybdenite occurring mainly at the top, the middle and the lower parts, respectively. The main metalliferous mineral of the Yuntoujie W-Mo deposit is wolframite, scheelite, molybdenite with minor amounts of chalcopyrite, sphalerite, and pyrite and gangue minerals including mainly quartz, muscovite, albite and tourmaline. The Yuntoujie ore bearing intrusion underwent greisenization and tourmalinization.

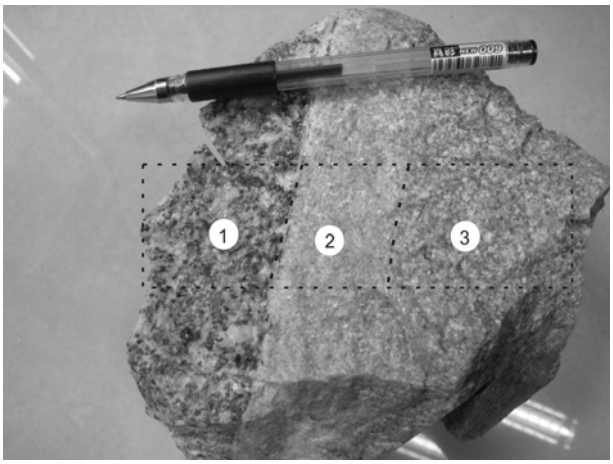

Figure 2 Photos showing the chilled contact line between the early stage batholith and late stage intrusion. 1, Early stage batholith; 2, chilled zone between the early stage batholith and late stage intrusion; 3, late stage intrusion.

2 Samples and analytical methods

We collected six molybdenite samples from small ore specimens (~1 kg) from the ore body "number one" in the Yuntoujie ore field (Figure 1(c)). The molybdenite were then magnetically separated and handpicked under a binocular microscope to ensure the purity was more than 99%. Re-Os isotope analyses were carried out in the Re-Os Laboratory, Guangzhou Institute of Geochemistry, Chinese Academy of Sciences. Each weighed sample was loaded in a Carius tube through a thin neck long funnel. This analytical procedure is described in detail by Sun et al. [30]. The Os-Re isotope ratios were determined using an X7 inductively coupled plasma mass spectrometer. The Re-Os isochron age was calculated with the program ISOPLOT. The decay constant used in the age calculation is $\lambda^{187}\mathrm{Re} = 1.666\times10^{-11}\ \mathrm{a}^{-1}$.

Zircon separates were collected from relatively small rock specimens (1 kg) with the least alteration. Standard separation techniques were applied, including jaw splitting, crushing in a swing mill, desliming in water, density separation in tetrabromoethane and methylene iodide, magnetic separation by isodynamic separator and finally with handpicking. Zircon grains were then mounted in epoxy and polished. Cathodoluminescent (CL) images and optical microscopy were used to select least fractured and inclusion-free zircons for analysis. Zircon analyses were performed in an inductively coupled plasma mass spectrometry (ICP-MS) laboratory at the Guangzhou Institute of Geochemistry, Chinese Academy of Sciences.

Laser ablation (LA) was conducted with a RESOlution M-50 Excimer laser operated at a constant energy of 80 mJ, with repetition rate of 8 Hz and a spot size of 31 μm diameter [31]. A mixed Ar-He carrier gas transported the ablated material from the sample cell into a flow homogenizer to an Agilent 7500a ICP-MS. Data were acquired for 20 s with the laser turned off and for a further 40 s with the laser turned on. Data exclusion is on the basis of three criteria.

Firstly, data that were more than 10% discordant were not used in age determinations. Secondly, spectra were examined for inclusions. Analyses with anomalously high La and/or high P values suggest that an apatite inclusion might have been intersected. These data were therefore discarded [32,33]. Thirdly, probability plots were used to examine the data. Cumulative probability plots have a nonlinear scale on the *x*-axis that was calibrated to represent a normal distribution as a straight line of a positive slope. Old U-Pb outliers (lying above the projection of the straight line) were interpreted to be inherited grains and young U-Pb outliers (lying below the line) were attributed to lead loss [32,33]. The U-Pb ages of the main population are obtained by removing grains from both ends of the main population until the tails had a gradient equal to or lower than the main population at both ends of the spectrum. The U-Pb age determined in this way was interpreted to be the cooling or crystallization age of the intrusion. Generally, this reduces the population MSWD $\leqslant$2.0.

3 Results and discussion

Zircon LA-ICP-MS data of rock samples from the early stage complex batholith and late stage ore bearing intrusion are listed in Tables 1 and 2. Concordia and probability plots are shown in Figure 3 and Re-Os isotope compositions are listed in Table 3.

3.1 Zircon LA-ICP-MS U-Pb age of the southwestern Miaoershan-Yuchengling complex batholith

Figure 4 shows that the analyzed zircons have well-developed oscillatory zoning and our analyses revealed relatively high Th/U ratios (0.10–0.24) (Tables 1 and 2). This indicates that the zircon grains are magmatic in origin. The main population zircon U-Pb age was interpreted as the crystallization age of the magmatic rocks.

The 25 zircon grains from the sample (YSD-1) collected from the Miaoershan-Yuechenling complex batholith were analyzed using LA-ICP-MS. Three data with more than 10% discordant values were discarded. Two zircon grains had LA-ICP-MS U-Pb ages of 450.7±15.6 Ma and 1378.8± 34.7 Ma respectively, and the remaining 20 zircon grains had U-Pb ages varying from 211 to 245 Ma. The two zircon grains with much older U-Pb ages were interpreted to be inherited zircon grains and therefore were not used for age determination. The other 20 zircon grains gave U-Pb ages of 225.0 ± 4.8 Ma with MSWD = 5.5. The population MSWD is greater than 2, suggesting that it may contain indiscernible subtle inheritance or Pb loss [32]. Based on the shape of the probability plot in Figure 3(a) (inset), one older outlier and four younger outliers were attributed to inheritance and Pb loss, respectively. The other 14 zircon grains gave a main population U-Pb age of 228.7 ± 4.1 Ma, with MSWD = 2.49. The zircon main population U-Pb age is taken as the crystallization age of the batholith. Our new zircon U-Pb age indicates that the southwestern domain of the Miaoershan-Yuechenling complex batholith was emplaced during the Indosinian period, other than the previous suggested Caledonian period [10]. This conclusion is very important for understanding the formation processes and evolution of the granitoids and related mineralization in the western Nanling ore belt.

3.2 Zircon LA-ICP-MS U-Pb age of the Yuntoujie ore-bearing granite

We analyzed 25 zircon grains for the Yuetoujie ore bearing granite and 3 data points with more than 10% discordant values were discarded. Four analyses with ages varying from 318 to 430 Ma were interpreted as inherited zircon grains. The other 18 zircon grains with ages ranging from 202 to 251 Ma have a main population age of 232.5 ± 8.7 Ma, with MSWD = 11.5 (Figure 3(b)) processed using ISOPLOT. As the main population MSWD value was much greater than 2, we processed that data using our probability plot. Based on the shape of the plot (Figure 3(b), inset) the analyzed zircon data can be divided into two groups. Group 1 contained 8 analyzed points and has a main population U-Pb age of 216.8 ± 4.9 Ma, with MSWD = 1.44. Group 2 contained 9 analyzed points and had a main population age of 243.0 ± 5.8 Ma, with MSWD = 2.62 (Figure 3(b) inset).

The well-developed oscillatory zonings of the group 1 zircon grains (Nos. 2, 3, 5, 8, 14, 19, 21 and 23, also in Figure 4, sample Y-21) indicate that the zircons were magmatic in origin. The Yuntoujie ore bearing intrusive rock had a chilled contact with the Miaoershan-Yuechenling batholith (Figure 2), suggesting that the ore bearing granite was emplaced after crystallization and cooling of the Miaoershan-Yuechenling batholith. The group 1 zircon age (216.8 ± 4.9 Ma, MSWD = 1.44), was less than the age of the batholiths and is interpreted to represent the emplaced age of the Yuntoujie intrusive rock associated with W-Mo mineralization. Our new zircon U-Pb age suggests that the Yuntoujie intrusive rock was also formed in the Indosinian period rather than the previously suggested Yanshanian period [34].

The group 2 zircons from the Yuntoujie intrusive rocks had an U-Pb age of 243.0 ± 5.8 Ma, with MSWD = 2.62. The well-developed oscillatory zoning and complete crystal forms of the group 2 zircon grains (Nos. 1, 9, 13, 16, 17, 20, 22, 24 and 25, also in Figure 4, sample Y-21), together with their relatively high Th/U (0.1–1.5) also indicate they are magmatic rather than metamorphic in origin [35–37]. The group 2 zircon grains also lack overgrowth rims which are often observed around residual zircon grains that have suffered from magmatism. For the group 2 zircons we interpret them to have been captured from the deep part of the Miaoershan-Yuechenling batholith during the ascension of the Yuntoujie magma. This group's zircon U-Pb age (243.0 ±

Table 1 Zircon LA-ICP-MS composition of the southwestern part of the Miaoershan-Yuechenling batholith[a)]

No.	U (ppm)	Atomic Th/U	$^{207}Pb/^{235}U$	±1s.e.	$^{206}Pb/^{238}U$	±1s.e.	$^{208}Pb/^{232}Th$	±1s.e.	$^{207}Pb/^{235}U$ age (Ma)	±1s.e.	$^{206}Pb/^{238}U$ age (Ma)	±1s.e.	$^{208}Pb/^{232}Th$ age (Ma)	±1s.e.	Concordance (%)
YSD-1-01	396	0.87	0.21920	0.01706	0.03365	0.00059	0.01065	0.00042	201.2	14.2	213.4	3.7	214.1	8.4	94
YSD-1-02	2027	0.14	0.26656	0.01218	0.03623	0.00046	0.01385	0.00065	239.9	9.8	229.4	2.9	277.9	12.9	95
YSD-1-03	412	0.93	0.95183	0.06211	0.08854	0.00275	0.03689	0.00136	679.1	32.3	546.9	16.3	732.3	26.6	78(omitted)
YSD-1-04	708	0.21	0.23682	0.01375	0.03533	0.00062	0.01136	0.00063	215.8	11.3	223.8	3.9	228.4	12.6	96
YSD-1-05	425	0.49	0.23650	0.01913	0.03511	0.00094	0.01091	0.00060	215.5	15.7	222.4	5.9	219.3	11.9	96
YSD-1-06	1588	0.15	0.25531	0.01719	0.04015	0.00094	0.01024	0.00057	230.9	13.9	253.8	5.8	205.9	11.4	90
YSD-1-07	650	0.52	0.24826	0.02022	0.03473	0.00061	0.01127	0.00081	225.2	16.4	220.1	3.8	226.6	16.2	97
YSD-1-08	370	0.39	0.52015	0.04127	0.07242	0.00260	0.02932	0.00149	425.3	27.6	450.7	15.6	584.0	29.2	94
YSD-1-09	677	0.38	0.22311	0.01434	0.03379	0.00051	0.01019	0.00053	204.5	11.9	214.2	3.2	205.0	10.7	95
YSD-1-10	240	1.05	0.23520	0.02254	0.03332	0.00088	0.01000	0.00052	214.5	18.5	211.3	5.5	201.2	10.4	98
YSD-1-11	191	1.58	0.25521	0.03755	0.03579	0.00118	0.01226	0.00065	230.8	30.4	226.7	7.3	246.3	13.0	98
YSD-1-12	854	0.23	0.24926	0.01621	0.03757	0.00065	0.01150	0.00068	226.0	13.2	237.7	4.1	231.1	13.5	94
YSD-1-13	571	1.27	0.22740	0.01615	0.03575	0.00078	0.01127	0.00042	208.0	13.4	226.5	4.8	226.5	8.4	91
YSD-1-14	163	1.03	0.26838	0.03292	0.03872	0.00111	0.01167	0.00067	241.4	26.4	244.9	6.9	234.5	13.4	98
YSD-1-15	2072	0.24	0.39085	0.02511	0.03980	0.00065	0.02275	0.00160	335.0	18.3	251.6	4.0	454.8	31.7	71(omitted)
YSD-1-16	641	1.52	0.26652	0.01763	0.03542	0.00072	0.01273	0.00059	239.9	14.1	224.4	4.5	255.6	11.8	93
YSD-1-17	406	0.58	0.24251	0.02334	0.03683	0.00085	0.01191	0.00072	220.5	19.1	233.2	5.3	239.3	14.4	94
YSD-1-18	439	0.32	0.24255	0.03130	0.03552	0.00079	0.01910	0.00124	220.5	25.6	225.0	4.9	382.5	24.7	97
YSD-1-19	726	0.20	0.25453	0.02166	0.03674	0.00070	0.01165	0.00072	230.3	17.5	232.6	4.3	234.2	14.4	98
YSD-1-20	416	0.81	3.36003	0.22873	0.23848	0.00667	0.07087	0.00418	1495.1	53.3	1378.8	34.7	1598.2*	129.6	91
YSD-1-21	780	0.16	0.27694	0.02240	0.03836	0.00078	0.01544	0.00108	248.2	17.8	242.7	4.8	309.6	21.6	97
YSD-1-22	644	0.22	0.26152	0.02309	0.03504	0.00069	0.01289	0.00097	235.9	18.6	222.0	4.3	258.9	19.4	93
YSD-1-23	534	1.05	0.18877	0.01927	0.03391	0.00072	0.00987	0.00047	175.6	16.5	215.0	4.5	198.6	9.4	79(omitted)
YSD-1-24	877	0.23	0.24700	0.01925	0.03397	0.00071	0.01236	0.00069	224.1	15.7	215.3	4.4	248.2	13.8	95
YSD-1-25	683	0.22	0.23864	0.02230	0.03397	0.00068	0.00952	0.00068	217.3	18.3	215.4	4.2	191.5	13.6	99

a) If U-Pb age is more than 1000 Ma, $^{207}Pb/^{206}Pb$ age was used.

Table 2 Zircon LA-ICP-MS composition of the Yuntoujie mineralized intrusion in the Miaoershan-Yuechenling batholith

Sample No.	U(ppm)	Atomic Th/U	$^{207}Pb/^{235}U$	±1s.e.	$^{206}Pb/^{238}U$	±1s.e.	$^{208}Pb/^{232}Th$	±1s.e.	$^{207}Pb/^{235}U$ age (Ma)	±1s.e.	$^{206}Pb/^{238}U$ age (Ma)	±1s.e.	$^{208}Pb/^{232}Th$ age (Ma)	±1s.e.	Concordance (%)
Y-21-01	707	0.25	0.27357	0.02639	0.03770	0.00081	0.01641	0.00110	245.5	21.0	238.5	5.1	329.0	21.8	97
Y-21-02	517	0.28	0.22622	0.02308	0.03390	0.00074	0.01221	0.00123	207.1	19.1	214.9	4.6	245.3	24.5	96
Y-21-03	128	1.46	0.22037	0.04512	0.03190	0.00112	0.01010	0.00066	202.2	37.6	202.4	7.0	203.2	13.3	99
Y-21-04	269	1.07	0.45598	0.04558	0.06349	0.00150	0.02182	0.00137	381.5	31.8	396.8	9.1	436.4	27.1	96
Y-21-05	669	0.40	0.22732	0.02533	0.03453	0.00086	0.01271	0.00110	208.0	21.0	218.8	5.4	255.3	21.9	94
Y-21-06	464	0.65	0.82755	0.07824	0.03666	0.00104	0.04386	0.00729	612.3	43.5	232.1	6.5	867.5	141.1	9
Y-21-07	516	1.12	0.46887	0.04056	0.06033	0.00225	0.01758	0.00122	390.4	28.0	377.6	13.7	352.2	24.1	96
Y-21-08	694	0.34	0.24178	0.02186	0.03437	0.00077	0.01135	0.00070	219.9	17.9	217.9	4.8	228.1	13.9	99
Y-21-09	1995	2.24	0.28532	0.02024	0.03804	0.00071	0.01547	0.00115	254.9	16.0	240.7	4.4	310.3	22.9	94
Y-21-10	339	1.51	0.42283	0.04432	0.06318	0.00161	0.02035	0.00111	358.1	31.6	394.9	9.7	407.2	22.0	90
Y-21-11	1173	0.46	0.43644	0.03490	0.05065	0.00152	0.02753	0.00643	367.7	24.7	318.5	9.3	548.9	126.5	85 (omitted)
Y-21-12	1388	0.18	0.28537	0.01865	0.04073	0.00082	0.01097	0.00063	254.9	14.7	257.3	5.1	220.5	12.6	99
Y-21-13	3513	0.10	0.26550	0.01536	0.03902	0.00071	0.01150	0.00064	239.1	12.3	246.7	4.4	231.2	12.8	96
Y-21-14	317	0.42	0.23488	0.02295	0.03356	0.00090	0.01033	0.00077	214.2	18.9	212.8	5.6	207.7	15.3	99
Y-21-15	160	1.11	0.53848	0.06507	0.06885	0.00225	0.02214	0.00145	437.4	43.0	429.2	13.6	442.7	28.7	98
Y-21-16	2370	0.09	0.26333	0.01720	0.03767	0.00068	0.01943	0.00173	237.3	13.8	238.4	4.2	388.9	34.3	99
Y-21-17	3120	0.09	0.30297	0.01931	0.03857	0.00084	0.01727	0.00146	268.7	15.1	243.9	5.2	346.0	29.0	90
Y-21-18	744	0.24	0.29349	0.02392	0.04307	0.00095	0.01119	0.00083	261.3	18.8	271.8	5.9	224.9	16.7	96
Y-21-19	1178	0.70	0.23862	0.01942	0.03364	0.00070	0.00996	0.00072	217.3	15.9	213.3	4.4	200.2	14.4	98
Y-21-20	191	0.74	0.32703	0.06050	0.03964	0.00126	0.02481	0.00288	287.3	46.3	250.6	7.8	495.3	56.7	86 (omitted)
Y-21-21	851	0.43	0.24072	0.02148	0.03564	0.00074	0.01167	0.00094	219.0	17.6	225.8	4.6	234.4	18.9	96
Y-21-22	276	0.83	0.28196	0.03275	0.04068	0.00101	0.01161	0.00080	252.2	25.9	257.0	6.2	233.3	16.0	98
Y-21-23	621	0.28	0.24312	0.02213	0.03481	0.00076	0.01623	0.00115	221.0	18.1	220.6	4.7	325.4	22.9	99
Y-21-24	914	0.37	0.24576	0.02133	0.03719	0.00110	0.01036	0.00067	223.0	17.4	235.4	6.8	208.4	13.4	94
Y-21-25	3535	0.21	0.24956	0.02129	0.03694	0.00076	0.01005	0.00054	226.2	17.3	233.8	4.7	202.1	10.7	96

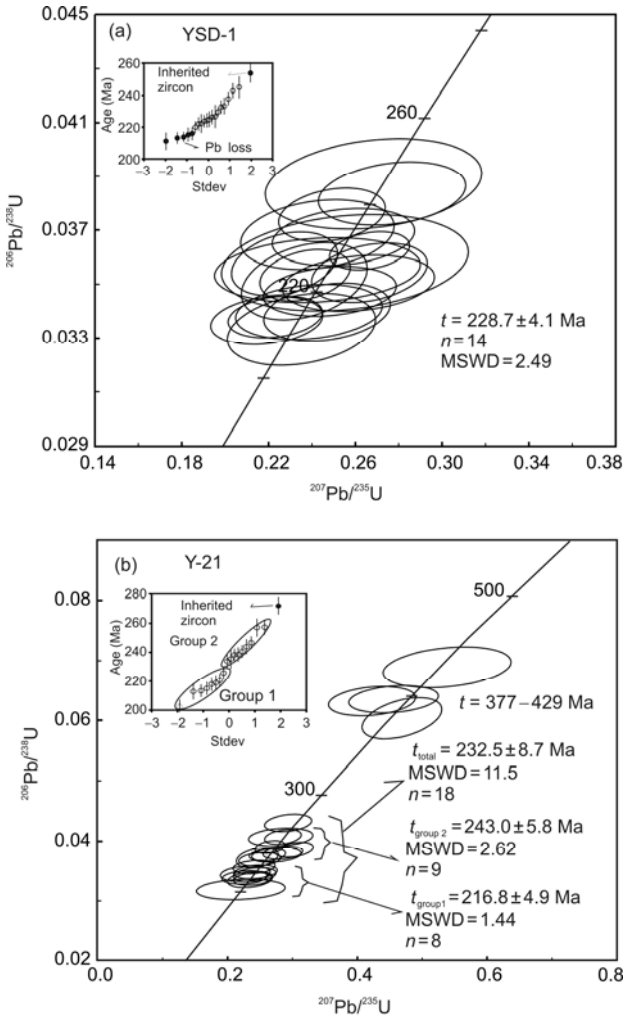

Figure 3 The concordia plots showing the U-Pb analyses of the Miaoershan-Yuechenling complex pluton (a) and the Yuntoujie ore bearing intrusion (b). The data in these plots have been culled of excessively scattered and discordant analyses following the criteria described in the text. Insets show the probability plots.

5.8 Ma) is also relatively older than the zircon U-Pb age from the sample YSD-1 (228.7 ± 4.1 Ma, MSWD = 2.49). It is suggested that the some part of the Miaoereshan batholith in the deep position was emplaced at about 243.0 ± 5.8 Ma. Based on our new zircon U-Pb data, we conclude that the southwestern domain of the early stage Miaoershan-Yuechenling batholith underwent two pulses of magmatic events, one pulse at ~228.7 ± 4.1 Ma and the other pulse at ~243.0 ± 5.8 Ma.

3.3 The Re-Os isochron age of the Yuntoujie W-Mo deposit

The Yuntoujie molybdenite samples have low concentrations ranging from 0.76 to 2.96 μg/g of Re (Table 3). This is much lower than those from the molybdenite in porphyry Cu-Mo deposits from other parts of the world, suggesting that the source of ore-forming material is crustal in origin. Six molybdenite samples have model ages ranging between 218 to 220 Ma. Six samples define a Re-Os isochron, with an age of 216.8 ± 7.5 Ma, MSWD = 11.3 (Figure 5). The model ages and isochron age of molybdenite are concordant with each other and within error.

The molybdenite Re-Os isochron age (216.8 ± 7.5 Ma) and the group 1 zircon U-Pb age (216.8 ± 4.9 Ma, MSWD = 1.44) agrees well within error suggesting that the data is precise. The W-Mo mineralization is genetically related to Yuntoujie intrusive rocks. This suggests both the Yuntoujie granite and the closely associated W-Mo mineralization were formed during the Indosinian tectono-magmatic event.

3.4 Formation of ore deposits around the Miaoershan-Yuechenling complex pluton and ore prospecting targets

Many ore deposits occurred in the contact zone around the Miaoershan-Yuechenling complex pluton and adjacent areas, forming an ore rich belt around the complex pluton (Figure 1). The element association of deposits around the Miaoershan-Yuechenling show systematic variations. Most W-Mo-Sn deposits occurred in the inner contact zone with more Pb-Zn-Cu deposits in the outer contact zone or in the adjacent strata.

The Miaoershan-Yuechenling complex pluton was formed by multi-magmatic events. Analysing which magmatic event that was genetic related to mineralization is essential for understanding the relationship between the Mesozoic magmatic evolution and the formation of the deposits. Thus, constraints on ore prospecting targets around the Miaoershan-Yuechenling complex pluton can be made.

Table 3 Re-Os compositions of molybdenite from the Yuntoujie W-Mo deposit

Sample No.	Weight (g)	Re (μg/g)	±σ	^{187}Re (μg/g)	±σ	^{187}Os (ng/g)	±σ	*t* (Ma)	Δ*t* (Ma)
Y-09	0.4000	0.76564	0.00252	0.48123	0.00159	1.71451	0.00959	213.5	1.4
Y-16	0.3382	1.57602	0.00338	0.99059	0.00213	3.61228	0.0025	218.5	0.5
Y-16-1	0.4576	1.18588	0.00443	0.74537	0.00279	2.66141	0.00494	213.9	0.9
Y-16-1R	0.4568	0.81967	0.00207	0.5152	0.0013	1.88217	0.00273	218.9	0.6
Y-16-2	0.3012	1.89849	0.00517	1.19328	0.00325	4.37612	0.00707	219.7	0.7
Y-22	0.1813	2.96345	0.00925	1.86265	0.00582	6.61547	0.00925	212.8	0.7

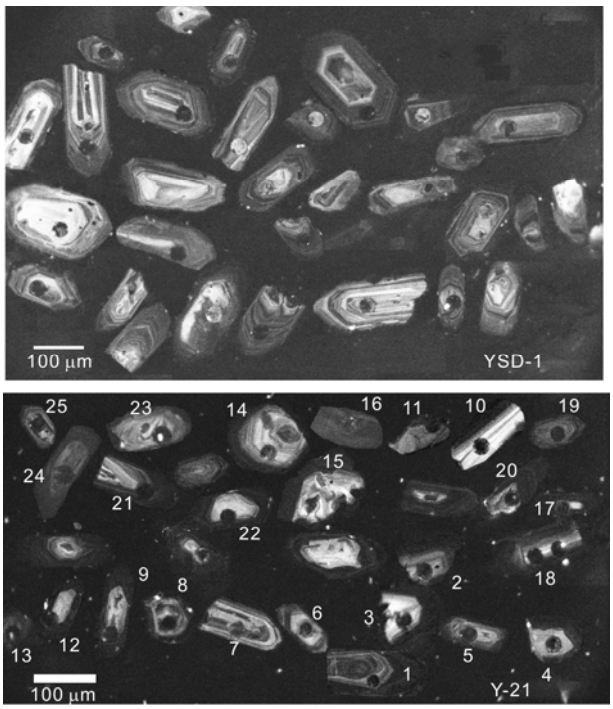

Figure 4 CL photos of zircon from the Miaoershan-Yuechenling complex pluton. YSD-1, Early stage complex pluton; Y-21, the Yuntoujie ore bearing intrusion. The zircon number in Y-21 corresponds to its number in Table 1.

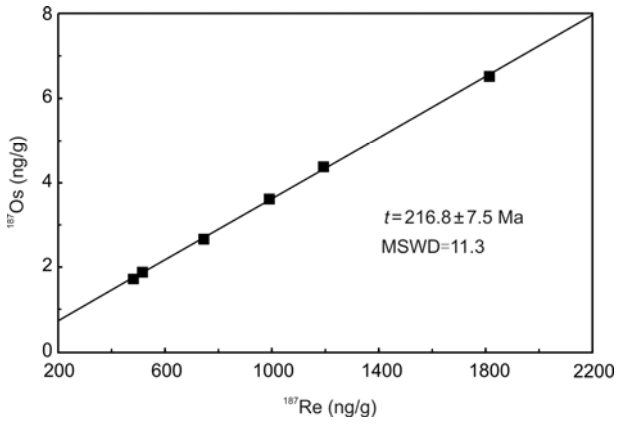

Figure 5 Re-Os isochron age of molybdenite from the Yuntoujie W-Mo deposit.

There is less work examining the relationship between the deposits around the Miaoershan-Yuechenling complex pluton and magmatic activities. Most of the local mine companies argued that the deposits around the Miaoershan-Yuechenling complex pluton owe their origin to the early stage Miaoershan-Yuechenling batholith. Most of deposits around the Miaoershan-Yuechenling complex pluton have W-Sn (Mo) element association and high temperature alteration such as greisenization, suggesting they are related to magmatic hydrothermal activities. Magmatic hydrothermal deposits are genetic related to an aqueous volatile phase exsolved from silicate melts [32,38–46] or fluids in equilibrium with silicate melts. If the silicate melts underwent mineralization processes during the ascending and crystallization of the melts, the aqueous volatile phase resolved from the melts should have reacted with the adjacent country rocks. An ore-forming element anomaly would have developed in the contact zone between the intrusive rocks and country rocks. No alteration was observed in the contact zone between the southwestern Miaoershan-Yuechenling granitoid batholith and the country rocks in the region of the Ziyuan County. Furthermore, there are no ore-forming element anomalies along the three geochemical exploration profiles that traverse the inner and outer contact zone of the Miaoershan-Yuechenling granitoid batholith (in submission). We therefore argue against the Miaoershan-Yuechenling granitoid batholith undergoing a mineralization processes during its formation. The deposits around the Miaoershan-Yuechenling complex pluton are closely associated with late stage magmatic activities, and the Re-Os isotope and zircon U-Pb ages reveal that the Yuntoujie W-Mo deposit in the southwestern domain of the Miaoershan-Yuechenling owes its origin to late stage intrusive activity, rather than early stage batholith. It is reasonable to conclude that the deposits around the Maioershan-Yuechenling complex pluton are genetic related to the late stage magmatic activities, rather than the early stage batholith.

Since the Maioershan-Yuechenling batholith is not genetically related to the deposits in its inner and/or outer contact zone, why then are there many deposits occurring in the contact zone, forming an ore-rich zone around the batholith? We have attributed this to the geological environment as follows: (1) the contact zone between the batholith and adjacent rocks provided favorable channels for the ascending of the late stage melts and volatile phase exsolved from late stage silicate melts and (2) the abrupt change in lithology in the contact zone between the batholith and country rocks was easy for reaction of magmatic related fluids with the country rocks, which resulted in the precipitation of ore-forming elements.

There are many Pb-Zn deposits (or occurrences) in the inner or outer contact zone of the Miaoershan-Yuechenling complex pluton. It is well known that the forming temperature of the Pb-Zn deposits is usually lower than those of W-Sn deposits associated closely with late stage intrusions. If Pb-Zn mineralization is not far from the W-Sn mineralization, the Pb-Zn and W-Sn mineralization may have originated from the same magmatic ore-forming system. In this case, the Pb-Zn mineralization would be located in the outer zone of the magmatic ore-forming system. If only Pb-Zn mineralization occurred in the region of the contact zone or adjacent region, the Pb-Zn mineralization might occur in the upper portion of the magmatic ore-forming system. In this case, attention should be paid to the suggestion that felsic intrusions are related to W-Mo mineralization in the much deeper location of the Pb-Zn mining region.

3.5 Indosinian mineralization and ore prospecting targets in South China

The Nanling region is well known for its granite related W-Sn-Be-Nb-Ta-REE deposits. Most of the previous work has focused on the Yanshaninan granite and related deposits [3–7,12–15] but there is less work on the Indosinian granite and its related mineralization. South China underwent both Indosinian and Yanshanian tectono-magmatic events in the Mesozoic period and it is proposed that the regional deformation was closely related to collisions and accretions of terrains in Southeast Asia during the Indosinian orogeny [47,48]. The Eastern Tethys Ocean closed at ~245 Ma when the Sibumasu block collided with Indochina-South China blocks during a period ranging from 258 ± 6 Ma to 243 ± 5 Ma [47–50]. The South China block collided with the North China block during the Indosinian orogeny, which resulted in the formation of the East Asian plate [43,51–54]. The Indosinian orogeny had great impact on the crustal tectonic evolution in South China [53]. In addition to our Indosinian ages of the southwestern part of the Miaoershan-Yuechenling batholith and late stage muscovite granite, the flowing lines such as the sedimentary environment mutation observed between the Permian and Triassic period in South China [54], the Indosinian granite found in Fujian, Hunan, Jiangxi, Guangdong, Hainan provinces, Guangxi Zhuang Autonomous Region (Guangxi for short) in China and the Indosinian metamorphism found in Zhejiang and Taiwan provinces (Table 4), indicate that South China underwent extensive Indosinian toctono-magmatic events.

W-Sn-Be-Nb-Ta-REE mineralization associated with the Yanshanian granite is widely distributed in South China, which forms one of the most important rare metals and REE ore belts in the world. The extensive development of the rare metals and REE deposits related to the Yanshanian granite suggests that the South China base is rich in these elements. Felsic melts resulting from the melting of the South China base triggered by the Indosinian orogeny could

Table 4 Indosinian isotope ages of rocks and mineralization in South China

Rocks or deposits	Isotope age	Reference
Luxi complex in southern Jingxi-northern Guangdong	239 ± 5 Ma (zircon LA-ICP-MS)	[55]
Xiazhuang complex in southern Jingxi-northern Guangdong	236 ± 8 Ma (zircon LA-ICP-MS)	[55]
Exiantang Sn-deposit in Jingxi	231.4 ± 2.4 Ma (muscovite $^{40}Ar/^{39}Ar$ plateau age)	[56]
Wuliting intrusion in Daji Mountain, Jingxi	238.9 ± 1.5 Ma (zircon SHRIMP U-Pb)	[57]
Baimianshi granite in Jingxi	249.9 ± 1.3 Ma (Rb-Sr isochron)	[58]
Darongshan intrusion in southeastern Guangxi	233 ± 5 Ma (zircon SHRIMP)	[59]
Jiuzhou intrusion in southeastern Guangxi	230 ± 4 Ma (zircon SHRIMP)	[59]
Taima intrusion in southeastern Guangxi	236 ± 4 Ma (zircon SHRIMP)	[59]
Limu deposit in northeast Guangxi	214.1 ± 1.9 Ma (muscovite $^{40}Ar/^{39}Ar$)	[60]
Miaoershan-Yuechengling batholith in northeastern Guangxi	243.0 ± 5.8 Ma, 228.7 ± 4.1 Ma (zircon LA-ICP-MS)	this work
Yuntoujie W-Mo ore-bearing granite in the Miaoershan-Yuechengling batholith in northeast Guangxi	216.8 ± 4.9 Ma (zircon LA-ICP-MS)	this work
Yuntoujie W-Mo deposit in northeast Guangxi	216.8 ± 7.5 Ma (molybdenite Re-Os)	this work
Hehuaping Sn deposit in southern Hunan	224 ± 1.9 Ma (molybdenite Re-Os isochron)	[61]
Weishan monzonitic granite in Hunan	244 ± 4 Ma (zircon SHRIMP)	[62]
Guandimiao intrusion in Hunan	239 ± 3 Ma (zircon SHRIMP)	[62]
Granite from the Baima Mountain in Hunan	243 ± 3 Ma (zircon SHRIMP)	[62]
Longyuaba intrusion in southern Jingxi-northern Guangdong	241.0 ± 5.9 Ma, 241.0 ± 1.3 Ma, 210.9 ± 3.8 Ma (zircon LA-ICP-MS)	[63]
Granite in the eastern Zhuguangshan	204 to 235 Ma (zircon SHRIMP)	[58]
Xiazhuang granitoid in northern Guangdong	228.0 ± 0.5 Ma (zircon SHRIMP)	[58]
Syenite in southwestern Fujian	252 to 242 Ma (zircon SHRIMP)	[64]
Topaz bearing granite in western Fujian	226 Ma (zircon SHRIMP)	[65]
Hexi group plagioclase amphibolites in Jingning, Zhejiang	252 ± 5 Ma (metamorphic zircon SHRIMP)	[66]
Basic-ultrabasic rock in southwestern Zhejiang	Metamorphic event at 251 to 233 Ma	[67]
Nappe structure in Zhejiang	(P_3-T_1)	[68]
Taiwan	Metamorphism at 260 to 240 Ma	[69]
Syenite in Hainan	244 ± 7 Ma (zircon SHRIMP)	[70]

have exsolved volatile phases during the ascending and crystallization of the melts such as those of the Yanshanian granite. Once these volatile phases exsolved from the felsic melts the rare metals and REE will participate into the volatile phase, which favors the formation of the Indosinian granitoid related deposits. Our new set of zircon LA-ICP-MS U-Pb and Re-Os isochron data, together with previous isotope ages on the Exiantang Sn deposit in the southern Jiangxi province [56], Hehuaping Sn deposit in the south Hunan province [62] and Limu Sn-Nb deposit in eastern Guangxi [61] indicate that South China underwent an Indosinian ore-forming event. We conclude that South China had dynamic conditions for large-scale mineralization during the Indosinian orogeny.

Based on our results and discussion, we propose that South China underwent not only the well- known Yanshanian mineralization, but also the Indosinian mineralization in the Mesozoic period. Therefore, South China has great potential for the Indosinian mineralization than previously thought and more attention should be given to Indosinian ore prospecting in South China.

Because of density differences between the melts and their exsolved volatile phases, felsic melt derived mineralization occurred in the upper portion of the intrusions and their upper adjacent area. South China experienced a large denudation because of the large scale crust uplift caused by the collision of the Sibumasu block with Indochina-South China blocks during the Indosinian orogeny. The large scale outcrop of the Miaoershan-Yuechenling complex pluton also suggests that its upper portion had been denudated. Some part of mineralization associated with Indosinian complex pluton might have been completely denudated. The ore-prospecting targets of Indosinian mineralization therefore, should focus on late stage small Indosinian intrusions that occurred in the complex pluton such as the Yuntoujie muscovite granite or small intrusions that occurred in the strata in depression regions such as the Limu granite associated with Sn-Nb mineralization

4 Conclusions

(1) The southwestern part of the Miaoershan-Yuechenling complex pluton was composed mainly of stage granitoid batholith and late stage small intrusions. The early stage batholith has a zircon LA-ICP-MS U-Pb age of 228.7 ± 4.1 Ma, with MSWD = 2.49 and may have some relatively older magmatic activity with a zircon U-Pb age of 243.0 ± 5.8 Ma, with MSWD = 2.62. The late stage Yuntoujie ore bearing intrusion has a zircon LA-ICP-MS U-Pb age of 216.8 ± 4.9 Ma, with MSWD = 1.44. The Yuntoujie W-Mo deposit has a Re-Os isochron age of 216.8 ± 7.5 Ma, with MSWD = 11.3. The early stage batholith, late stage intrusions and the closely associated W-Mo mineralization were formed during the Indosinian orogeny.

(2) The deposits that occurred in the Miaoershan-Yuechenling complex pluton or in its contact zone were derived from late stage magmatic activities rather than the early batholith. Indosinian ore prospecting targets should focus in the Indosinian late stage intrusions in complex pluton or its contact zone.

(3) South China underwent not only the well-known Yanshanian rare metal and REE mineralization, but also the Indosinian mineralization and South China has much greater potential for the Indosinian ore prospecting than previously thought.

This work was supported by the Knowledge Innovation Program of Chinese Academy of Sciences (*KZCX1-YW-15-3*), *the Strategic Guiding Scientific and Ttechnologic Program of Chinese Academy of Sciences* (*XDA08130202*), *Three-dimensional Deep Exploration Technology for Mineral Resources and Experiment* (*SinoProbe-03-01*) *and the National Natural Science Foundation of China* (*41172080, 41121002*). *The co-operation and support of Shengyuan Mining Company greatly facilitated the field work for this study. Dr. Zhang Hong is thanked for the help with the isotope analyses. Two anonymous reviewers are also thanked for greatly improving the manuscript through their thoughtful and thorough reviews. This is contribution No. IS-1443 from GIGCAS.*

1 Institute of Geochemistry, Chinese Academy of Sciences. Geochemistry of Granitoids in South China (in Chinese). Beijing: Science Press, 1979. 1–285
2 Mo Z S, Ye B D, Pan W Z. Geology of Nanling Granite (in Chinese). Beijing: Geological Publishing House, 1980. 1–363
3 Geological Department of Nanjing University. Relationship between Different Age Granitoids and Mineralization in the South China (in Chinese). Beijing: Science Press, 1981. 1–395
4 Granite Research Group of Ministry of Geology and Mineralogy. Geology, Genesis and Mineralization of Granite in the South China (in Chinese). Beijing: Geological Publishing House, 1989. 1–259
5 Chen Y H, Pei R F, Zhang H L, et al. Geology of Non-ferrous Metal and Rare Metal Deposits Related to the Mesozoic Granite in the Nanling Region (in Chinese). Beijing: Geological Publishing House, 1989. 1–506
6 Hua R M, Chen P R, Zhang W L, et al. Metallogenic systems related to Mesozoic and Cenozoic granitoids in South China. Sci China Ser D-Earth Sci, 2003, 46: 816–829
7 Hua R M, Chen P R, Zhang W L, et al. Metallogeneses and their geoldynamic settings related to Mesozoic granitoids in the Nanling range (in Chinese). Geol J Chin Univ, 2005, 11: 291–304
8 Wang D H, Chen Y C, Li H Q, et al. Geological and geochemical features of the Furong tin deposit in Hunan and their significance for mineral prospecting (in Chinese). Reg Geol Chin, 2003, 22: 50–56
9 Zhu J C, Zhang P H, Xie C F, et al. The Huashan-Guposhan A-type granitoid belt in the western part of the Nanling Mountains: Petrology, geochemistry and genetic interpretations (in Chinese). Acta Geol Sin, 2006, 80: 529–542
10 Zhou X M. Petrogenesis of Late Mesozoic Granites and Dynamic Evolution of Lithosphere in Nanling Region (in Chinese). Beijing: Science Press, 2007. 1–386
11 Gilder S A, Gill J, Coe R S, et al. Isotopic and paleomagnetic constraints on the Mesozoic tectonic evolution of South China. J Geophys Res, 1996, 101: 16137–16154
12 Mao J W, Xie G Q, Li X F, et al. Mesozoic large scale mineralization and multiple lithospheric extensions in South China (in Chinese). Earth Sci Front, 2004, 11: 45–55
13 Mao J W, Xie G Q, Guo C L, et al. Spatial-Temporal distribution of Mesozoic ore deposits in South China and their metallogenic settings (in Chinese). Geol J Chin Univ, 2008, 14: 510–526

14 Liu Y H, Fu J M, Long B L, et al. He and Ar isotopic components of main tin deposits from central Nanling region and its signification (in Chinese). J Jilin Univ, 2006, 36: 774–781
15 Li H Q, Lu Y F, Wang D H, et al. Dating of the rock-forming and ore-forming ages and their geological significances in the Furong orefield, Qitian Mountain, Hunan (in Chinese). Geol Rev, 2006, 52: 113–121
16 Jiang S Y, Zhao K D, Jiang Y H, et al. New type of tin mineralization related to granite in South China: Evidence from mineral chemistry, element and isotope geochemistry (in Chinese). Acta Petrol Sin, 2006, 22: 2509–2524
17 Peng J T, Hu R Z, Bi X W, et al. $^{40}Ar/^{39}Ar$ isotopic dating of tin mineralization in the Furong deposit of Hunan province and its geological significance (in Chinese). Mineral Dep, 2007, 26: 237–248
18 Liang H Y, Xia P, Wang X Z, et al. Geology and geochemistry of the adjacent Changkeng gold and Fuwang silver deposits, Guangdong Province, South China. Ore Geol Rev, 2007, 31: 304–318
19 Sun W D, Ling M X, Ding X, et al. The genetic association of adakites and Cu-Au ore deposits. Int Geol Rev, 2011, 53: 691–703
20 Hu R Z, Bi X W, Zhou M F, et al. Uranium metallogenesis in South China and its relationship to crustal extension during the Cretaceous to Tertiary. Econ Geol, 2008, 103: 583–598
21 Li X H, Li W X, Li Z X. On the genetic classification and tectonic implications of the early Yanshanian granitoids in the Nanling Range, South China. Chin Sci Bull, 2007, 52: 1873–1885
22 Wang T G, Ni P, Sun W D, et al. Zircon U-Pb ages of granites at Changba and Huangzhuguan in western Qinling and implications for source nature. Chin Sci Bull, 2011, 56: 659–669
23 Guo S S, Li S G. Petrochemical characteristics of leucogranite and a case study of Bengbu leucogranites. Chin Sci Bull, 2009, 54: 1923–1930
24 Xie L, Wang R C, Chen J, et al. Primary Sn-rich titianite in the Qitianling granite, Hunan Province, southern China: An important type of tin-bearing mineral and its implications for tin exploration. Chin Sci Bull, 2009, 54: 798–805
25 Wang R C, Zhang W L, Lei Z H, et al. Zircon U-Pb dating confirms existence of a Caledonian scheelite-bearing aplitic vein in the Penggongmiao granite batholith, South Hunan. Chin Sci Bull, 2011, 56: 2031–2036
26 Wang F Y, Ling M X, Ding X, et al. Mesozoic large magmatic events and mineralization in SE China: Oblique subduction of the Pacific plate. Int Geol Rev, 2011, 53: 704–726
27 Xu W C, Zhang Y H, Liu Y B. Progression in geochronological study and scheme of chrono-classfication on the Miaoershan granite batholith (in Chinese). Acta Petrol Sin, 1994, 15: 332–337
28 Sun T. A new map showing the distribution of granites in South China and its explanatory notes (in Chinese). Reg Geol China, 2006, 25: 332–337
29 Wu J, Liang H Y, Lou F, et al. Result of applying routine secondary halo method to tungsten-molybdenum prospecting work in Yuntoujie area of Ziyuan County, Guangxi, and its significance (in Chinese). Mineral Dep, 2010, 29: 301–307
30 Sun Y L, Xu P, Li J, et al. A practical method for determination of molybdenite Re-Os age by inductively coupled plasma-mass spectrometry combined with Carius tube-HNO_3 digestion. Anal Methods, 2010, 2: 575–581
31 Tu X L, Zhang H, Deng W F, et al. Application of RESOlution *in-situ* laser ablation ICP-MS in trace element analyses (in Chinese). Geochimitia, 2011, 40: 83–98
32 Liang H Y, Campbell I H, Allen C M, et al. Zircon Ce^{4+}/Ce^{3+} ratios and ages for Yulong ore-bearing porphyries in eastern Tibet. Miner Dep, 2006, 41: 152–159
33 Harris C A, Allen C M, Bryan S E, et al. ELA-ICP-MS U-Pb zircon geochronology of regional volcanism hosting the Bajo de la Alumbrera Cu-Au deposit: Implications for porphyry-related mineralization. Miner Deposit, 2004, 39: 46–67
34 Guangxi Zhuang Autonomous Region Bureau of Geology and Mineral Resources. Regional Geological Memoirs of the Guangxi Zhuang Autonomous Region (in Chinese). Beijing: Geological Publishing House, 1985. 1–325
35 Rubatto D, Gebauer D, Compagnoni R. Dating of eclogite-facies zircons: The age of Alpine metamorphism in the Sosia-Lanzo Zone (Western Alps). Earth Planet Sci Lett, 1999, 167: 141–158
36 Hoskin P W O, Black L P. Metamorphic zircon formation by solid state recrystallization of protolith igneous zircon. J Metamorph Geol, 2000, 18: 423–439
37 Sun W D, Williams I S, Li S G. Carboniferous and Triassic eclogites in the western Dabie Mountains, east-central China: Evidence for protracted convergence of the North and South China Blocks. J Metamorph Geol, 2002, 20: 873–886
38 Liang H Y, Sun W D, Su W C, et al. Porphyry copper-gold mineralization at Yulong, China, promoted by decreasing redox potential during magnetite alteration. Econ Geol, 2009, 104: 587–596
39 Baker T, Achterberg E V, Ryan C G. Composition and evolution of ore fluids in a magmatic-hydrothermal skarn deposit. Geology, 2004, 32: 117–120
40 Heinrich C A, Günther D, Audétat A, et al. Metal fractionation between magmatic brine and vapor, determined by microanalysis of fluid inclusions. Geology, 1999, 27: 755–758
41 Heinrich C A, Driesner T, Stefánsson A, et al. Magmatic vapor contraction and the transport of gold from porphyry environment to epithermal ore deposits. Geology, 2004, 32: 761–764
42 Ulrich T, Günther D, Heinrich C A. Gold concentrations of magmatic brines and the metal budget of porphyry copper deposits. Nature, 1999, 399: 676–679
43 Lowenstern J B, Mahood G A, Rivers M L, et al. Evidence for extreme partitioning of copper into a magmatic vapor phase. Nature, 1991, 252: 1405–1409
44 Hedenquist J W, Lowenstern J B. The role of magmas in the formation of hydrothermal ore deposits. Nature, 1994, 370: 519–527
45 Shinohara H, Hedenquist J W. Constraints on magma degassing beneath the Far Southwest porphyry Cu-Au deposit, Philippines. J Petrol, 1997, 38: 1741–1752
46 Candela P A, Piccoli P M. Model ore-metal partitioning from melts into vapor and vapor/brine mixtures. In: Thompson J F H, ed. Magmas, Fluids and Ore Deposits. Mineral Assoc Can, 1995, 23: 101–127
47 Carter A, Roques D, Bristow C. Understanding Mesozoic accretion in Southeast Asia: Significance of Triassic thermotectonism (Indosinian orogeny) in Vietnam. Geology, 2001, 29: 211–214
48 Chung S L, Lo C H, Lan C Y. Collision between the Indochina and South China blocks in the Early Triassic: Implications for the Indosinian Orogeny and closure of eastern Paleotethys. In: AGU 1999 Fall Meeting. Washington D C: Eos T Am Geophys Union, 1999, 80: 1043
49 Zhang G W, Cheng S Y, Guo A L, et al. Mianlue paleo-suture on the southern margin of the Central Orogenic System in Qinling-Dabie with a discussion of the assembly of the main part of the continent of China (in Chinese). Reg Geol Chin, 2004, 23: 846–853
50 Li S G, Liu D L, Chen Y Z, et al. Time of the blueschist belt formation in central China (in Chinese). Chin J Geol, 1993, 28: 21–27
51 Sun W D, Li S G, Chen Y D. Timing of synorogenic granitoids in the South Qinling, central China: Constraints on the evolution of the Qinling-Dabie orogenic belt. J Geol, 2002, 110: 457–468
52 Ames L, Tilton G R, Zhou G. Timing of collision of the Sino-Korean and Yangtse cratons: U-Pb zircon dating of coesite-bearing eclogites. Geology, 1993, 21: 339–342
53 Ren J S, Niu B G, Liu Z G. Soft collision, superposition orogeny and polycyclic suturing (in Chinese). Earth Sci Front, 1999, 6: 85–93
54 Liu B J, Xu X S. Atlas of Paleogeography and Lithofacies of South China: Sinian-Trias (in Chinese). Beijing: Science Press, 1994. 1–188
55 Xu D X, Deng P, O'Reilly S Y. Single zircon LA-ICP-MS U-Pb dating of Guidong granite complex (SE China) and its petrogenetic significance. Chin Sci Bull, 2003, 48: 1328–1334
56 Liu S B, Wang D H, Chen Y C, et al. $^{40}Ar/^{39}Ar$ ages of muscovite from different type tungsten-bearing quartz veins in the Chong-Yu-You concentrated mineral area in Gannan region and its geological significance (in Chinese). Acta Geol Sin, 2008, 82: 932–939
57 Zhang W L, Hua R M, Wang R C, et al. Single zircon U-Pb isotopic age of the Wuliting granite in Dajishan area of Jiangxi, and its geo-

logical implication (in Chinese). Acta Geol Sin, 2004, 78: 352–358
58 Chen P R, Zhou X M, Zhang W L, et al. Petrogenesis and significance of early Yanshanian syenite-granite complex in eastern Nanling range. Sci China Ser D-Earth Sci, 2004, 34: 493–503
59 Deng X G, Chen Z G, Li X H, et al. Shrimp U-Pb zircon dating of the Darongshan-Shiwandashan granitoid belt in southeastern Guangxi, China (in Chinese). Geol Rev, 2004, 50: 462–432
60 Yang F, Li X F, Feng Z M, et al. $^{40}Ar/^{39}Ar$ dating of muscovite from greisenized granite and geological significance in Limu tin deposit (in Chinese). J Guilin Univ Tech, 2009, 29: 20–24
61 Cai M H, Chen K X, Qu W J, et al. Geological characteristics and Re-Os dating of molybdenites in Hehuaping tin-polymetallic deposit, southern Hunan province (in Chinese). Mineral Dep, 2006, 25: 263–268
62 Wang Y J, Fan W M, Liang X Q, et al. Shrimp zircon U-Pb geochronology of Indosinian granites in Hunan province and its petrogenetic implications. Chin Sci Bull, 2005, 50: 1259–1265
63 Zhang G M, Chen P R, Huan G G, et al. Single zircon LA-ICP-MS age of the Longyuanba pluton in the eastern Nanling region and geological implication. Acta Geol Sin, 2006, 80: 984–994
64 Wang Q, Li J W, Jian P. Alkaline syenites in eastern Cathaysia (South China): Link to Permian-Triassic transtension. Earth Planet Sci Lett, 2005, 230: 339–354
65 Zhao L, Yu J H, Wang L J, et al. Formation time of Hongshan topaz-bearing granite and its metallogenic potential prognosis (in Chinese). Mineral Deposit, 206, 25: 672–682
66 Chen D F, Li X H, Pan J M, et al. Metamorphic newly produced zircons, SHRIMP U-Pb age of amphibolite of Hexi Group, Zhejiang and its implications (in Chinese). Acta Mineral Sin, 1998, 18: 396–400
67 Xiang H, Zhang L, Zhou H W, et al. U-Pb zircon geochronology and Hf isotope study of the metamorphosed basic-ultrabasic rocks from metamorphic basement in southwestern Zhejiang: The response of the Cathaysia Block to Indosinian orogenic event. Sci China Ser D-Earth Sci, 2008, 38: 401–413
68 Xiao W J, He H Q. Early Mesozoic thrust tectonics of the northwest Zhejiang region (Southeast China). GSA Bull, 2005, 117: 945–961
69 Jahn B M, Chi W R, Yui T F. A Late Permian formation of Taiwan (Marbles from Chia-Li well No. 1): Pb-Pb Isochron and Sr isotopic evidence, and its regional geological significance. Geol Soc Chin, 1992, 193–218
70 Xie C F, Zhu J C, Zhao Z J, et al. Zircon SHRIMP U-Pb age dating of garnet-acmite syenite: Constraints on the Hercynian-Indosinian tectonic evolution of Hainan Island (in Chinese). Geol J Chin Univ, 2005, 11: 47–57